

# Determining Actual Aircraft Positions Relative to The Runway Using the Airborne Redar and Approach Navigation

Yuri Vladislavovich Likharev\* Vladimir Mikhailovich Nuzhdin\* Pavel Vladimirovich Sokolov\* Vasily Ivanovich Akhrameev\*\* and Marina Sergeevna Shelagurova\*\*\*

**Abstract :** The article deals with the scientific and technical problem off light safety for light aircraft performing domestic flights and general aviation aircraft (GAA) when approaching in low visibility conditions and in absence of an optical visibility using on-board software and hardware represented by the airborne short-range radar (ASRR), airborne computer and LCD display. ASRR basic technical features and functionality are introduced. The algorithms of determining the aircraft position relative to runway boundaries are described. It has been established that as a result of processing panoramic radar images (RI) obtained in the ASRR, the distance to the runway (RW) boundary and the aircraft heading angle relative to the runway direction can be measured, which allows to ensure safe aircraft landing in low visibility conditions and even in absence of an optical visibility through displaying necessary flight and navigation data in the LCD display. The first experimental results of ASRR tests performed on the IKARUS C42 light aircraft of CJSC Tehaviakompleks have been presented.

**Keywords:** Flight safety, airborne short-range radar, navigation, display, flight testing, measuring the distance and heading angle, aircraft landing.

## 1. INTRODUCTION

The Russian small aircraft market sector has been significantly growing in the last decade along with restoration of regular scheduled domestic flight and an increase in the volume of aviation operations, the potential demand for which is rather high due to large distances, poor road networks, increasing consumer purchasing power and aspiration of active consumers for mobility.

One of the serious problems of small aircraft (SA) safety, including both light and ultralight planes, is detecting terrains, other aircraft and ground vehicles, as well as boundaries of runways (RW) and taxi ways (TW) when approaching unprepared airfields in low visibility conditions and even in absence of an optical visibility, including night flights. The existing radar equipment cannot solve this problem as it cannot be installed in light aircrafts due to its large size and expensiveness. The solution suggested to solve this problem is using a new compact and low-cost airborne short-range radar (ASRR) on SA planes.

**The features distinguishing this ASRR from other radars are as follows:**

- High rate for obtaining data (similar to optic sensors);
- High distance resolution (about 1 m) and azimuthal resolution (1 degree or less);

\* Moscow Aviation Institute (National Research University), MAI 4, Volokolamskoye shosse, Moscow, 125993, Russian Federation

\*\* JSC "Tehaviakompleks" Garnaeva street, 2A, Gromov Flight Research Institute, Zhukovsky, Moscow region, 140182, Russian Federation

\*\*\* JSC "Ramenskoye Design Company", 2 Gurieva St., Ramenskoye, Moscow Region 140103, Russian Federation

- Small weight and size, low power consumption;
- Can be installed on a wide range of SA and unmanned aerial vehicle (UAV) aircraft;

The price for the above advantages is reasonable limitation of the ASRR range. Such radars are not presented in the market [1]. The issues of creating the ASRR meeting these requirements have been described in works [2-9] relating to an automotive radar and a fire helicopter [10].

## 2. BASIC ASRR TECHNICAL FEATURES

ASRR is a panoramic millimeter-wavelength radar consisting of two functional modules: *external*–radar type and *internal* – analog-to-digital type with a digital information exchange bus connected with a power cable. Figure 1 shows taking off of IKARUS C42 of CJSC Tehaviakompleks (Russia) with the installed ASRR, performed in test flights.



Fig. 1. IKARUS C42 with the installed ASRR during testing.

Basic technical features of the experimental ASRR model are shown in Table 1.

**Table 1. Basic ASRR technical features**

Instrumented range, m	20-1500
Range resolution, m	1.5 ÷ 3
Azimuthal resolution, degree	≤ 1
Operation frequency, GHz	39
Radiation power, mW	30-50
Antenna:	slotted waveguide
Antenna coverage sector in the azimuthal plane, degree	± 60
Antenna coverage sector in the elevation plane, degree	from 0 (up) to -12 (down)
Number of data points in a radar image	(256 × 512) per shot
Power consumption	< 100 W (12-24 V circuit)
Data updating speed, Hz	5 ÷ 10
Data output format	1 Gbit/s Ethernet
Radar weight (antenna + transceiver), kg	Not more than 10

**The above ASRR technical features and functionality ensure performance of the following tasks in low visibility conditions (dusk, fog, drizzle, snow, smoke etc.) :**

- Control of airspace for aerial objects (helicopters, airplanes, paragliders, etc.) and high surface facilities (transmitting towers, plant chimneys, high-rise buildings, etc.), and establishing coordinates of these objects.
- Generation of the detailed highly informative radar image of the surface (mapping) allowing to make navigation aircraft position fixation based on a radar map and search for a landing area.
- Detection of fixed obstacles and moving vehicles on the runway and TW when landing and taxiing.

The ASRR ensures generation of radar data obtained to be displayed on a pilot's multimode display in real time.

**In addition to structural issues, improvement of the automotive radar (airborne version of short-range radar was developed on its base) to provide aircraft safety must be made in two directions:**

1. Increasing the operating range (due to a higher speed of light aircraft, compared to a vehicle).
2. Creating algorithms for reprocessing of generated radar images (RI) in real time to ensure proper approach, driving on the runway and taxiways in low visibility conditions and in absence of an optical visibility.

The algorithms for detecting aircraft positions relative to runway boundaries and evaluation of its heading angle for pilot's adequate perception of the situation, as well as for interactive (or automated in case of UAV) aircraft control when landing are described below.

### 3. METHODOLOGY FOR DETERMINING AIRCRAFT POSITIONS RELATIVE TO THE RUNWAY

Geometrical relationships clarifying visibility procedures are shown in Figure 2.

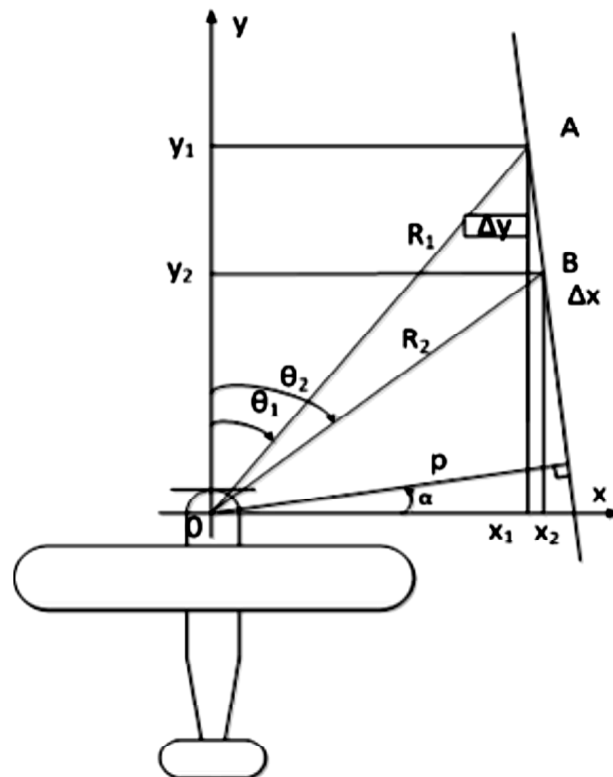


Fig. 2. Task geometry. Aircraft position when landing.

The antenna beam narrow in the azimuthal plane perform scanning, consistently taking the position characterized by the angle  $\Omega_{SC} t = \theta$ . Azimuth angles are counted from the OY axis left to right to the right runway boundary.

The delay time of a signal reflected from the runway boundary is measured for consistent beam positions  $\theta_1, \theta_2, \dots, \theta_n$ .

We introduce the algorithm allowing based on data obtained from the radar to determine the distance from the aircraft to the runway boundary. The radar makes measurements in the coordinate system (OXY) fixed with aircraft construction lines. The highly detailed radar image generated by the radar [5] allows to determine not only the distance to the runway boundary but also the angle characterizing aircraft orientation when landing in relation to the runway.

We assume that the runway boundary might be approximated with a straight line determined by the equation (1) in the coordinate system of the radar (the origin of the coordinate system is fixed with the aircraft).

$$x \cos \alpha + y \sin \alpha - p = 0 \quad (1)$$

where  $\alpha$  – angle between the runway boundary and the OY axis,  $p$  – distance from the boundary to the origin of the coordinate system,  $x$  and  $y$  – coordinates of an arbitrary point on the RI plane.

Figure 2 shows aircraft position when landing in the coordinate system fixed with aircraft construction lines. The runway boundary is indicated with line AB.

The radar scans the space in front of the aircraft and measures the range  $R$  and the angle  $\theta$  of obtained signals reflected from the runway boundary.

The equation characterizing the OA line in the XOY plane can be written in the form similar to (1):

$$x \cos \theta - y \sin \theta = 0 \quad (2)$$

“-” sign in equation (2) is provided due to the fact that samples of angle and are calculated in different directions.

The coordinates of point A – point of crossing of two straight lines, are defined from the simultaneous solution of (1) and (2):

$$\left. \begin{array}{l} \left\{ \begin{array}{l} y \cdot \sin(\alpha) + x \cdot \cos(\alpha) - p = 0 \\ y \cdot \sin(\alpha) + x \cdot \cos(\alpha) = 0 \end{array} \right\} \\ x_1 \frac{\begin{vmatrix} B_1 & C_1 \\ B_2 & 0 \end{vmatrix}}{\begin{vmatrix} A_1 & B_1 \\ A_2 & B_2 \end{vmatrix}} = \frac{p \cdot \sin \theta_1}{\sin(\theta_1 - \alpha)}; y_1 = \frac{\begin{vmatrix} C_1 & A_1 \\ 0 & A_2 \end{vmatrix}}{\begin{vmatrix} A_1 & B_1 \\ A_2 & B_2 \end{vmatrix}} = \frac{p \cdot \cos \theta_1}{\sin(\theta_1 - \alpha)} \end{array} \right\} \quad (3)$$

and thus the distance from the origin to the point A( $x_1, y_1$ ) is determined in the form:

$$R_1 = \sqrt{x_1^2 + y_1^2} = \frac{p}{\sin(\theta_1 - \alpha)} \quad (4)$$

As equations (3),(4) include unknown variables  $p$  and  $\alpha$ , the variables  $R_2$  and  $\theta_2$  must be measured once again and,

$$R_2 = \sqrt{x_2^2 + y_2^2} = \frac{p}{\sin(\theta_2 - \alpha)} \quad (5)$$

Thus, to determine these unknown parameters  $p$  and  $\alpha$ , the simultaneous solution of equations (4) and (5) is necessary.

If we take the ratio  $\Delta x / \Delta y$ , where:

$$\Delta x = x_2 - x_1 = R_2 \sin \theta_2 - R_1 \sin \theta_1 \quad (6)$$

$$\Delta y = y_2 - y_1 = R_2 \cos \theta_2 - R_1 \cos \theta_1 \quad (7)$$

the equation to calculate the required parameter  $\alpha$  will be as follows:

$$\alpha = \arctg \left( \frac{\Delta x}{\Delta y} \right) \cong \frac{R_2 \sin \theta_2 - R_1 \sin \theta_1}{R_2 \cos \theta_2 - R_1 \cos \theta_1} \quad (8)$$

The distance to the runway boundary  $p$  is calculated when substituting (6) and (7) in (4) and (5):

$$p = R_1 \sin(\theta_1 - \alpha) = R_2 \sin(\theta_2 - \alpha) \quad (9)$$

Measuring two distances  $R_1$  and  $R_2$  and corresponding angles  $\theta_1$  and  $\theta_2$  allows to determine the parameter  $\alpha$  calculated through equation (8) and characterizes the angle of aircraft axis deviation from the runway direction in the XOY plane, and the distance to its boundaries can be calculated using the formula (9).

#### 4. ALGORITHM FOR MEASURING THE DISTANCE TORUNWAY BOUNDARIES AND DETERMINING THEHEADING ANGLE

The above methods for measuring runway boundariesandheading angle are used in the multi-channel detector of the runway, the algorithm of whichis described below.

Each  $i$ -th channel of the detector is RI range section.

The task of measuring the distance torunway boundariesand determining the deviation angle is to determine the distance to the runway boundaryin all sounding directions  $\theta$  and to subsequently make statistical calculation of required parameters  $p$  and  $\alpha$ . This task can be divided into the following stages:

1. The range of the allowed valuesof  $p$  is set:  $p \in \left[ \frac{L_M}{2}, n_n L_n + \frac{L_M}{2} \right]$   $\alpha \in [-10^\circ, 10^\circ]$ . This range is selected based on priori data.
2. The angle  $\theta$  is expressed through radar technical features  $\theta = \theta_{\text{view}} \left( \frac{N}{N_{\text{TX}}} - \frac{1}{2} \right)$ , where  $\theta_{\text{view}}$  – scanning sector,  $N_{\text{TX}}$  – number of soundingperiods while monitoring the sector,  $N$  – RI azimuth section number.
3. Range search borders depend on the channel number

$$DR(N) = \frac{\Delta p}{\sin \left( \theta_{\text{view}} \left( \frac{N}{N_{\text{TX}}} - \frac{1}{2} \right) - \Delta \alpha \right)} \quad (10)$$

4. The azimuth coverage is divided into search sectors for the left and right runway boundary.

$$N \in \left( 0, \left( \arcsin \left( \frac{-p_{L_{\text{min}}}}{R_{\text{max}}} \right) + \alpha_{\text{max}} + \frac{\theta_{\text{view}}}{2} \right) \frac{N_{\text{TX}}}{\theta_{\text{view}}} \right) \cup \left( \left( \arcsin \left( \frac{p_{R_{\text{max}}}}{R_{\text{max}}} \right) + \alpha_{\text{min}} + \frac{\theta_{\text{view}}}{2} \right) \frac{N_{\text{TX}}}{\theta_{\text{view}}}, N_{\text{TX}} \right) \quad (11)$$

$$S_L = \left( 0, \left( \arcsin \left( \frac{-p_{L_{\text{min}}}}{R_{\text{max}}} \right) + \alpha_{\text{max}} + \frac{\theta_{\text{view}}}{2} \right) \frac{N_{\text{TX}}}{\theta_{\text{view}}} \right) \text{ – left boundary serach sector}$$

$$S_R = \left( \left( \arcsin \left( \frac{p_{R_{\text{max}}}}{R_{\text{max}}} \right) + \alpha_{\text{min}} + \frac{\theta_{\text{view}}}{2} \right) \frac{N_{\text{TX}}}{\Delta \theta_{\text{CK}}}, N_{\text{TX}} \right) \text{ – right boundary serach sector}$$

As a result,the area,wherethe distance torunway boundariesis measured (Figure 3), is selected in the radar image.

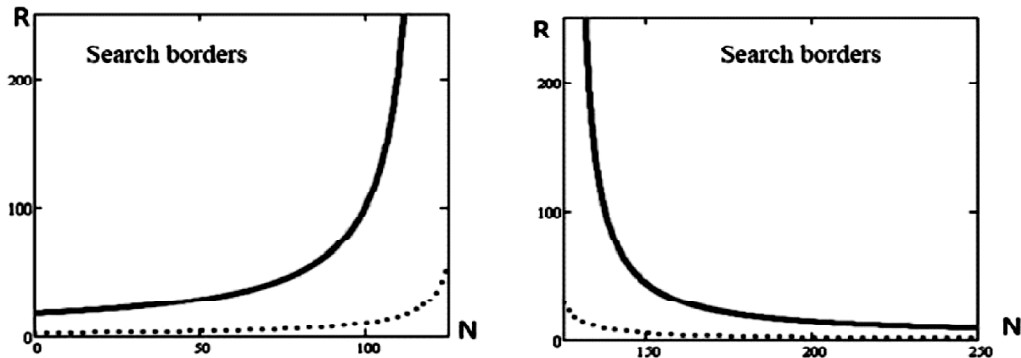


Fig. 3. Search area forrunway boundaries (The proximal search area boundary is identified with dotted lines, the distal boundary – with the solid line).

1. The values of  $p_L$ ,  $p_R$ ,  $\alpha$  are calculated using estimates of distances to the runway boundary in channels (R).

$$\begin{cases} p_R(N_i, R_i) = R_i \sin \left( \theta_{\text{view}} \left( \frac{N_i}{N_{3u}} - \frac{1}{2} \right) + \alpha \right) \\ p_L(N_i, R_i) = -R_i \sin \left( \theta_{\text{view}} \left( \frac{N_i}{N_{3u}} - \frac{1}{2} \right) + \alpha \right) \\ \alpha(N_i, R_i) = \arctan \left( \frac{R_i \sin \left( \theta_{\text{view}} \left( \frac{N_i}{N_{\text{TX}}} - \frac{1}{2} \right) \right) - R_{i-1} \sin \left( \theta_{\text{view}} \left( \frac{N_{i-1}}{N_{\text{TX}}} - \frac{1}{2} \right) \right)}{R_i \cos \left( \theta_{\text{view}} \left( \frac{N_i}{N_{\text{TX}}} - \frac{1}{2} \right) \right) - R_{i-1} \cos \left( \theta_{\text{view}} \left( \frac{N_{i-1}}{N_{\text{TX}}} - \frac{1}{2} \right) \right)} \right) \end{cases}$$

6. Calculation of average values  $m$  and mean square deviations  $\sigma$  for estimated values  $p$  and  $\alpha$ .

$$m[p] = \frac{1}{n} \sum_{n=1}^m p(N_n, R_n); M[\alpha] = \frac{1}{n} \sum_{n=1}^m \alpha(N_n, R_n) \quad (13)$$

$$\sigma[p] = \sqrt{\frac{1}{n} \sum_{n=1}^m (p(N_n, R_n) - M[p])^2} \quad \sigma[\alpha] = \sqrt{\frac{1}{n} \sum_{n=1}^m (\alpha(N_n, R_n) - M[\alpha])^2} \quad (14)$$

7. Anomalous point filtration.

Since the runway width is constant, we can make the  $R'$  sample from the  $R$  array based on the following criterion  $p_i - M[p] < \sigma$

$$\overline{R} \xrightarrow{p_i - M[p] < \sigma} \overline{R'} \quad (15)$$

8. Determining extrapolated values  $p$  and  $\alpha$  to estimate these values in the next RI frame

$$p \in [M[p] - n \cdot \sigma[p], M[p] + n \cdot \sigma[p]] \quad (16)$$

$\alpha \in [M[\alpha] - n \cdot \sigma[\alpha], M[\alpha] + n \cdot \sigma[\alpha]]$ , to determine  $p$  and  $\alpha$  in the next frame.

Thus, as a result of RI processing, the distance to the runway boundary (radial outbound or radial distance), runway width and aircraft heading angle relative to the runway direction can be measured in the radar, which allows to ensure safe landing in low visibility conditions and even in absence of an optical visibility.

## 5. RADAR EXPERIMENTAL DATA

The airborne short-range radar generates a highly detailed radar image (RI). The RI samples obtained through the ASRR in live experiments in summer, fall and winter 2015 are shown in Figures 4 and 5.

Figure 4 shows synchronous video and radar runway images with the autogyro taxiing for take off (shown as a yellow circle). The image was generated from the surface. There is also a stationary vehicle (shown as a red circle) and a person (shown as a blue circle) in the RI. Detecting stationary and moving objects using the ASRR, including such small objects as a person, allows to significantly reduce the risk of flight accidents.

Figure 5 shows synchronous video and radar runway images obtained in the air when flying over the runway. The RI clearly shows the runway boundary, buildings, etc. The aircraft position and the heading angle can be estimated using this radar data, but a relevant algorithm should be used for this purpose.

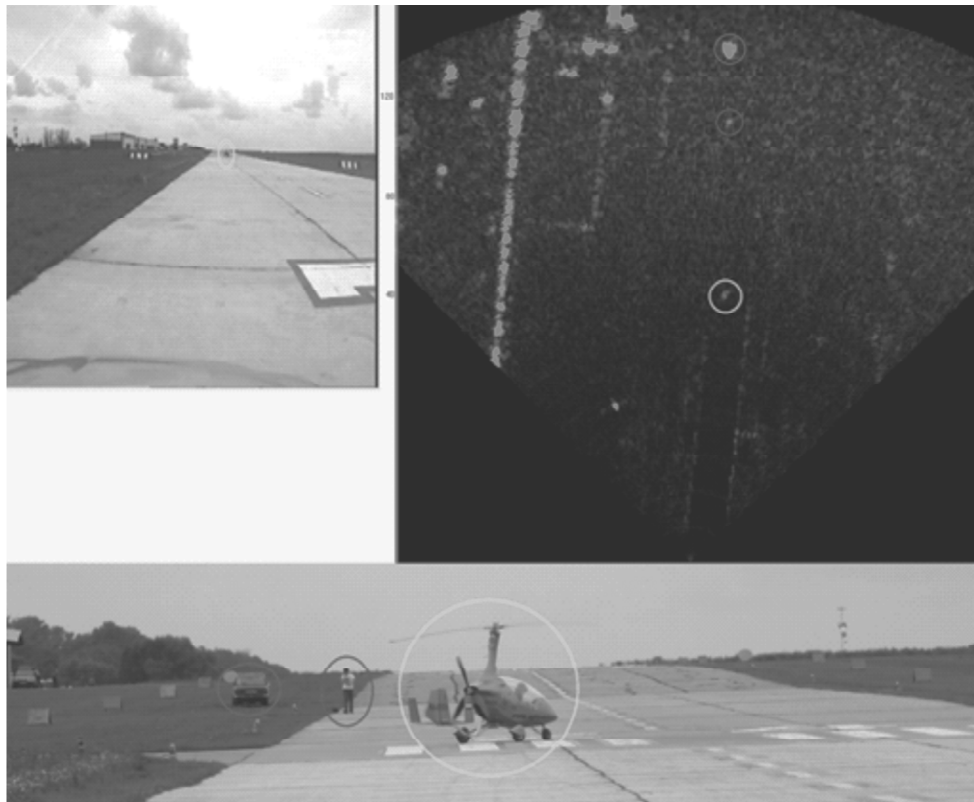


Fig. 4. Radar and video image of the runway with the autogyro obtained from the surface.

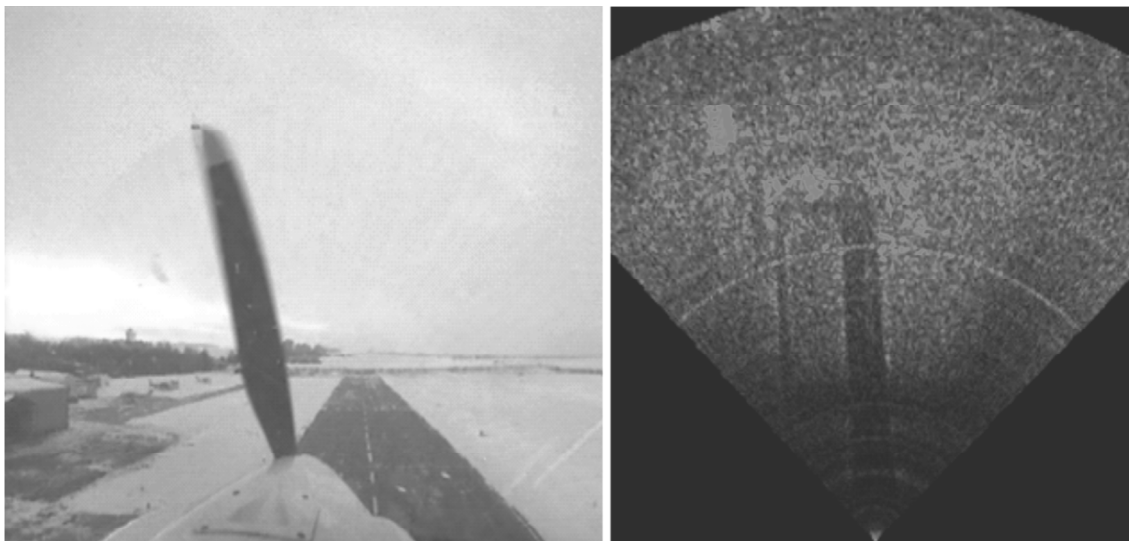


Fig. 5. RI and optical image of the runway obtained in flight.

## 6. FORMAT OF DISPLAYING NAVIGATION DATA TO THE CREW WHEN APPROACHING

For the purpose of navigation and pilot age when approaching, various indication options can be used, which can both display a computerized runway image and display coordinates of the runway or gli depth relative to the aircraft in the LCD display using special symbols including directing signals. Both of the above provide the pilot with the data required for safe aircraft control when approaching and landing in low visibility conditions and in absence of an optical visibility [11].

Figure 6 shows the symbols of the display mode in the window “Navigation to the runway threshold”, which displays aheading angle to the runway threshold, radial distance to the runway threshold, landing heading and current linear deviation (LD) from the runway axis to the pilot.

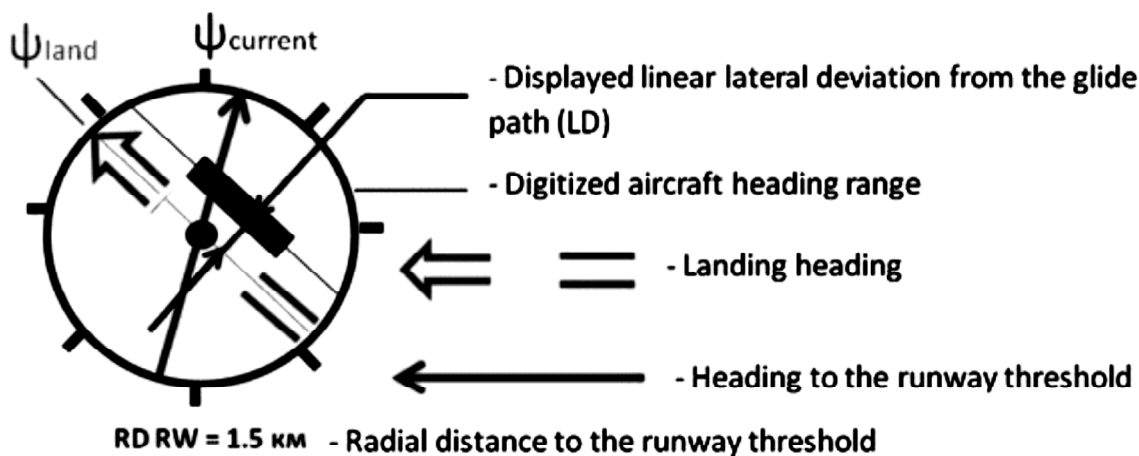


Fig. 6. Window “Navigation to the runway threshold” implemented in a display mode in the LCD display when approaching.

At that, the parameters of graphic display of the LD value from the runway axis are limited depending on the actual LD according to the chart shown in Figure 7.

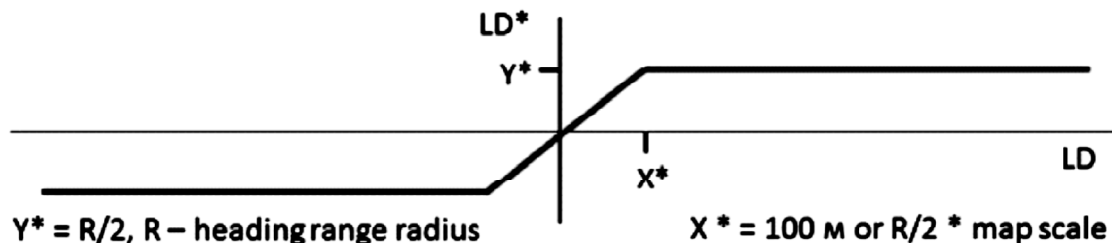


Fig. 7. Limited physical display of the LD value from the runway axis.

The following parameters for displaying “control commands” in the LCD display can be provided in the command mode of landing on the air fields elected:

- intended track;
- landing heading;
- current linear deviation (LD) from the runway axis;
- desired trajectory deviation in a vertical plane;
- desired trajectory deviation in a horizontal plane.

Transition to a landing mode is performed either manually or automatically under the following conditions:

- difference between the current track and landing heading of the runway does not exceed  $\pm 60^\circ$  (to be adjusted based on further testing);
- LD from the runway axis is  $\leq 1.5 \text{ km}$  (to be adjusted based on further testing);
- distance to the runway threshold is within 300 – 1500 m (to be adjusted based on further testing);
- current relative height ( $H_{rel}$ ) depending on the distance to the runway is within the following range:  $D_{rw} \cdot \text{tg} 1^\circ \leq H_{rel} \leq D_{rw} \cdot \text{tg} \theta$ , where  $\theta$  – glide path slope value multiplied by 1.1. H

**Two approach modes are provided in a complex :**

- using signals generated in a complex based on data of the air channel and satellite navigation system (SNS) with the computerized runway image on the LCD display;
- using signals generated from the ASRR.

This ensures pre-landing maneuvering and generation of similar commands of deviations from the predetermined track and glide path angles, similar to the airborne complex operating mode when using landing tools (ILS, MLS, PRMG).



**Note :** MLS ensures the preset azimuth and elevation)

The airborne complex generated the following control signals in the landing mode:

- calculated deviations  $\varepsilon_h$  from the desired track;
- calculated deviations  $\varepsilon_g$  from the preset glide path slope angle;
- distance to the runway threshold.

The aircraft control in the vertical plane is performed based on the deviation of a horizontal position bar generated with the signal and the control in a horizontal plane is performed based on the deviation of a vertical bar with the signal .

The calculated values of a deviation from the preset track and glide path slope angle values, and the distance to the runway threshold are calculated in an airborne complex using two methods in ascending priority:

- based on the data of integrated processing of coordinates, speed, height (if there is SNS when working in a differential and non-differential mode), relative barometric altitude from the air data system (ADS) and radio altitude from the RA (after passing front runway threshold),
- based on the data obtained from imaging sensors and modified to geographic coordinates.

The calculations are made taking into account runway centerline coordinates, glide path slope angle, runway length and PZ approach track (database information).

Upon reaching the height of 50 m (to be adjusted based on further testing) in the automatic landing mode the airborne complex displays the “Decision Height” feature in the LCD display. Conditions and transition to the “Reapproach” mode will be additionally described.

When using the computer vision system (CVS) the airborne complex can generate an improved synthetic image providing the crew with the runway image more complete form with additional information on distances to special markers on the runway based on data from the radar [11].

To generate the runway 3D image, special scientific software (SS) of the converter has been developed, which allows to convert data from ARINC 424 format and from shape files into binary files with the airborne specialized structure [12]. Integration of runway ranges into 3D-ranges of terrain and application of a special texture imitating the surface of a real runway to runway ranges, as shown in Figure 8, are performed in the synthesized vision mode SS.

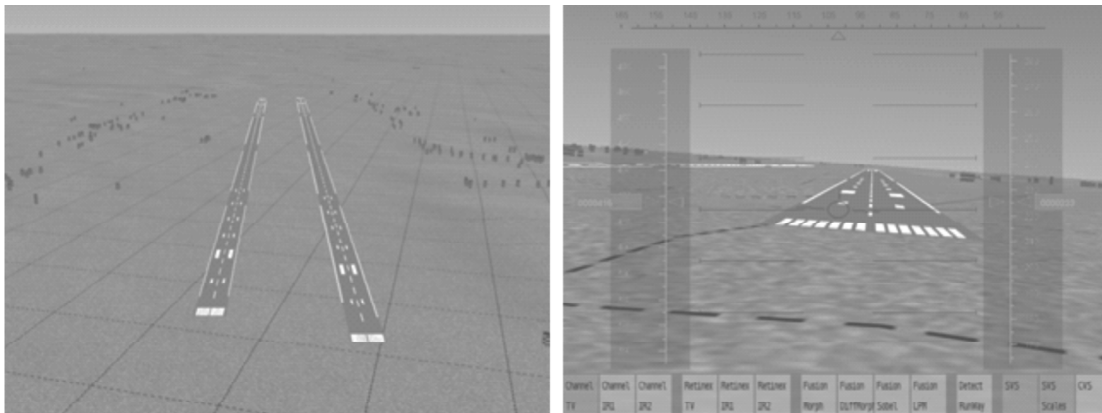


**Fig. 8. Example of runway synthesized image.**

The ergonomic evaluation of results obtained showed that display of relative runway position data with generation of 3D runway image helps the crew to navigate in space which positively affects the psychophysical state of the crew and thus improves flight safety [13].

Figure 9 below shows display formats implemented in the approach and landing mode based on data from the ASRR, database information and data from the SNS with application of the window “Navigation on the runway threshold”.

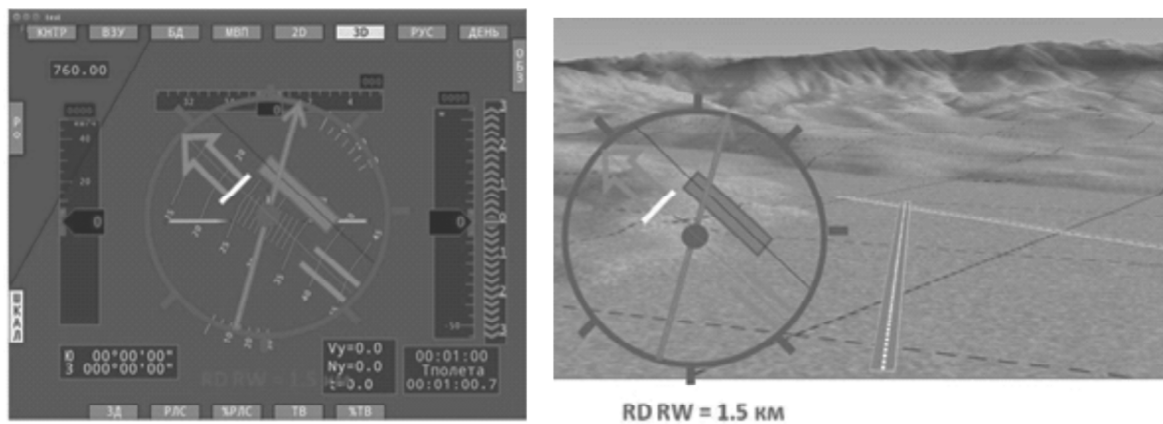


Fig. 9. Window "Navigation on the runway threshold".

The display of the reference approach trajectory in the directing mode of approach on the airfield selected is shown in Figure 10.

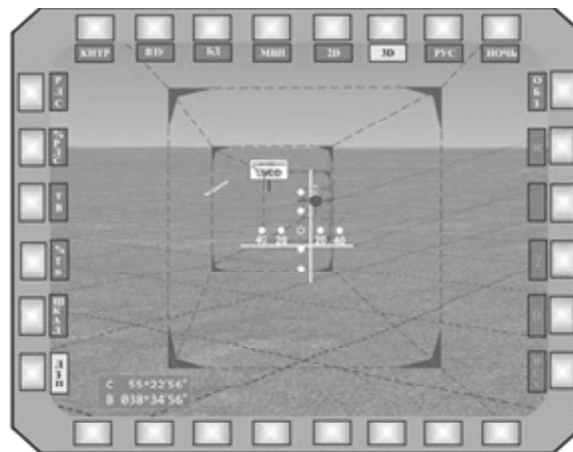


Fig. 10. Display of the reference trajectory, command bars and velocity vector on the 3D shot.

## 7. CONCLUSION

This article has demonstrated that in order to ensure safety of the low-level flight and landing of the light SA aircraft in low visibility conditions and in absence of an optical visibility the panoramic forward vision radar with high space resolution must be used onboard the aircraft.

It has been proved that it is technically possible to install the airborne short-range radar (ASRR) on board the small aircraft (SA). The experimental ASRR model has been created by the group of specialists from the Moscow Aviation Institute (National Research University).

It has been shown that as a result of processing radar images (RI) obtained in the ASRR, the distance to the runway boundary and heading angle of the aircraft relative to runway landing heading can be measured, which allows to ensure safe landing in low visibility conditions and in absence of an optical visibility.

During flight testing, the experimental ASRR model has proved to be able to detect moving objects, stationary obstacles, runway boundaries and taxi ways (TW). Flight testing has pre-determined implementation of the ASRR in automated light SA aircraft control systems.

For the purpose of control automation, the multi-channel tracking unit measuring the distance to runway boundaries and the heading angle has been developed using priori data on the nature of the runway boundary, as a distributed target.

For the purpose of navigation and pilotage, the indication option has been introduced which is displayed in the LCD display and provides a pilot with data required for safe aircraft control when approaching.

The results provided in this article have been obtained when performing applied research sponsored by the Ministry of Education and Science of the Russian Federation under Agreement No.14.579.21.0051 of September 16, 2014.

The applied research unique identifier is RFMEFI57914X0051.

## 8. REFERENCES

1. Skolnik, M.I. (Ed.). (2014). *Spravochnik po radiolokatsii* [Radar Handbook]. Moscow: TECHNOSFERA.
2. Rastorguev, V., Nuzhdin, V., Sidorov, N., Sulimov, Y. et al. (2000). Sistema radiovideniya "AvtoRadar". Upravlenie dvizheniem avtomobilya [Autoradar Radio-Wave Imaging System. Vehicle Movement Control]. *Elektronika*, 5.
3. Shelukhin, O.I. (1989). *Radiosistemy blizhnego deystviya* [Short Range Radio Systems]. Moscow: Radio i svyaz'.
4. Ananenkov, A.E., Nuzhdin, V.M., Rastorguev, V.V., & Skosyrev, V.N. (2013). Osobennosti otsenki kharakteristik obnaruzheniya v RLS maloy dal'nosti [Peculiarities of Radar Detection Performance Evaluation of Short-Range Radio Technology]. *Radiotekhnika*, 11, 35-38.
5. Ananenkov, A., Konovaltsev, A., Nujdin, V., Rastorguev, V., & Sokolov, P. (2008). Characteristics of Radar Images in Radio Vision Systems of the Automobile". In *Proceeding of International Conference on Transparent Optical Networks – ICTON-MW'08, Marrakech, Morocco, December 11-13th, 2008*.
6. Ananenkov, A., Konovaltsev, A., Kukhorev, A., Nujdin, V., & Rastorguev, V. (2009). Features of Formation of Radar-Tracking and Optical Images in a Mobile Test Complex of Radiovision Systems of the Car. *Journal of Telecommunications and Information Technology*, 1, 29-33.
7. Ananenkov, A.E., Nuzhdin, V.M., Rastorguev, V.V., Sokolov, P.V., & Schneider, V.B. (2014). System Radiovision for Movement Automation of the Vehicles Column. In *Proceeding of 16<sup>th</sup> International Conference on Transparent Optical Networks – ICTON'2014, Graz, July 6th-10th* (pp. 1-6).
8. Nuzhdin, V.M., Rastorguev, V.V., & Schneider, V.B. (2014). Issledovanie tochnosti opredeleniya mestopolozheniya avtomobilya otnositel'no granits dorogi [Investigation of Accuracy in Determining Vehicle Position Relative to Road Edges]. *Zhurnal radioelektroniki*, 8.
9. Ananenkov, A.E., Bui Chi Thanh, Gerasimov, L.A., Rastorguev, V.V., & Sokolov, P.V. (2015). Evaluation of Vehicle Movement Speed by the means of the Automobile Radar Data. In *Proceeding of 17th International Conference on Transparent Optical Networks – ICTON'2015, Budapest, July 5th-9th* (pp. 1-5).
10. Ananenkov, A.E., Karpyshev, A.V., Morozov, G.A., Nuzhdin, V.M., Rastorguev, V.V., & Schneider, V.B. (2014). Mikrovolnovyy datchik opredeleniya distantsii vertoletnoy sistemy pozharotusheniya [Microwave Sensor Determining the Distance of the Helicopter Fire-Fighting System]. *Izvestiya VUZov. Aviatcionnaya tekhnika*, 4.
11. Akhrameev, V.I., Babichenko, A.V., Sokolov, S.M., & Zemlyany, E.S. (2015). Flight Safety Support System Development for Low-altitude Flights of Light Aircraft. *Biosciences, Biotechnology Research Asia*, 12(03), 1-8.
12. Shelagurova, M.S. (2014). Issledovanie metodov polucheniya informatsii o vzletno-posadochnykh polosakh s tsel'yu otobrazheniya v sistemakh sintezirovannogo videniya [Investigation of Methods for Obtaining Information on Runway to be Displayed in Synthetic Vision Systems]. *Aviakosmicheskoe priborostroenie*, 11, 12-20.
13. Shelagurova, M.S., Janjgava, G.I., & Sazonova, T.V. (2012). Intellektual'naya podderzhka ekipazha v rezhime zakhoda na posadku vozdushnogo sudna [Intelligent Crew Support in Aircraft Approaching]. *Voprosy oboronnoy tekhniki. Seriya* 9, 5(257), 4-14.